Stem Cell Reports
Article

ISSCR

OPEN ACCESS

WNT16B enhances the proliferation and self-renewal of limbal epithelial cells via CXCR4/MEK/ERK signaling

Songjiao Zhao,[1] Xichen Wan,[1] Yiqin Dai,[1,2,3] Lan Gong,[1,3,4,*] and Qihua Le[1,2,3,4,*]
[1]Department of Ophthalmology, Eye, Ear, Nose & Throat Hospital of Fudan University, No. 83 Fenyang Road, Shanghai 200031, China
[2]Research Center, Eye, Ear, Nose & Throat Hospital of Fudan University, Shanghai 200031, China
[3]Myopia Key Laboratory of Ministry of Health, Eye, Ear, Nose & Throat Hospital of Fudan University, Shanghai 200031, China
[4]Senior author
*Correspondence: 13501798683@139.com (L.G.), qihuale_eent@163.com (Q.L.)
https://doi.org/10.1016/j.stemcr.2022.03.001

SUMMARY

Culture of limbal epithelial cells (LECs) provides the principal source of transplanted limbal stem cells (LESCs) for treatment of limbal-stem-cell deficiency. Optimization of the culture conditions for *in-vitro*-expanded LECs will help to create a graft with an optimized quality and quantity of LESCs. This study aimed to investigate the effects of WNT16B on LECs and corneal wound healing and the underlying mechanism. Treatment with exogenous WNT16B increased the proliferative capacity and self-renewal of LECs in the cultures. We further revealed that C-X-C chemokine receptor type 4 (CXCR4) was vital for the effects of WNT16B, and activation of CXCR4/MEK/ERK signaling was pivotal in mediating the effects of WNT16B on LECs enriched for LESCs. The stimulatory effect of WNT16B on corneal epithelial repair was confirmed in a mouse corneal-wound-healing model. In summary, WNT16B enhances proliferation and self-renewal of LECs via the CXCR4/MEK/ERK signaling cascade and accelerates corneal-epithelial wound healing.

INTRODUCTION

Limbal epithelial stem cells (LESCs) in the basal layer of the epithelium of the corneoscleral limbus are adult stem cells with high proliferative and self-renewal potentials (Schermer et al., 1986). The ability of LESCs to maintain the integrity and transparency of the corneal epithelium is essential for normal visual function. Destruction of the limbus, which occurs with ocular burns and in severe ocular diseases, may lead to loss of LESCs and limbal-stem-cell deficiency (LSCD) (Haagdorens et al., 2016). In such cases, the cornea is invaded by conjunctival epithelial cells, and this is accompanied by chronic inflammation, persistent corneal-epithelial defects, neovascularization, and loss of vision (Le et al., 2018).

Transplantation of *in-vitro*-expanded LECs has successfully restored the function of the limbus and therefore is a promising technique for treating LSCD (Rama et al., 2010; Trounson and McDonald, 2015). A tiny biopsy from the healthy limbus of a patient or cadaveric tissue is cultured *in vitro* on a substrate to form LEC sheets enriched for LESCs, which are then transplanted into the eyes of patients with LSCD (Grueterich et al., 2003). It can be used in the treatment of both unilateral and bilateral LSCD. More importantly, *in vitro* LEC cultivation could minimize the exposure to allogeneic antigens, decrease the incidence of graft rejection, and improve the prognosis, especially in bilateral LSCD cases (Ghareeb et al., 2020; Li et al., 2007). Rama et al. (2010) showed that the success rate is higher after transplantation of a cell sheet containing more than 3% P63α^{+} LESCs. Therefore, the clinical success of therapy using cultured LECs is primarily dependent on the quality of cultures, especially the number of functional LESCs in cultured cell sheets.

Optimization of the *in-vitro*-culture conditions to maintain the number and function of LESCs may increase the success rate of transplantation and improve the clinical outcome. Many studies have sought to ameliorate and optimize the culture conditions via various means, including improving the culture substrate and adding exogenous complementary factors such as epidermal growth factor (EGF), insulin, and cholera toxin to the culture system (Grueterich et al., 2003; Hogerheyde et al., 2016; Trosan et al., 2012; Yu et al., 2016).

WNT ligands are a family of lipid-modified secreted proteins that regulate stem-cell activities, including self-renewal, proliferation, differentiation, survival, and polarity. There are 19 members of the WNT family. Some activate the canonical WNT signaling pathway, some activate non-canonical WNT signaling pathways, and others activate both types of signaling pathways (Clevers et al., 2014). WNT16, which activates both canonical and non-canonical WNT signaling pathways, participates in bone formation, skin homeostasis, and hair growth by regulating the proliferation and renewal of stem cells in these locations (Kandyba et al., 2013; Kim et al., 2019; Mendoza-Reinoso and Beverdam, 2018; Meyers et al., 2018; Teh et al., 2007; Tong et al., 2019). WNTs and WNT signals are present in the LESC niche and are pivotal for homeostasis of LESCs (González et al., 2019; Gouveia et al., 2019; Nakatsu et al., 2011; Ouyang et al., 2014). Although WNT16B is enriched at the limbus (Nakatsu et al., 2011), its role in

maintenance of the normal LESC population and corneal-epithelial renewal is unclear. Based on previous findings that WNT16B protein is predominantly expressed in the suprabasal and basal layers of the limbus epithelium and colocalizes with △Np63, a stemness marker of LESCs (Kawasaki et al., 2006; Nakatsu et al., 2011), we hypothesized that WNT16B might play a pivotal role in proliferation and stemness maintenance of LESCs.

In this study, expression of WNT16B in the normal human cornea and limbus was observed, and its location was identified. To investigate the effect of WNT16B on LESCs, we treated *in-vitro*-cultured LECs with WNT16B, investigated their growth and phenotype, and explored the underlying molecular mechanism. Moreover, we established a mouse corneal-epithelial wound-healing model and explored the effect of WNT16B on corneal-epithelial wound repair *in vivo*. We provide the first evidence that WNT16B enhances proliferation and self-renewal of LESCs and is a promising novel tool in translational medicine and cell therapy for treatment of LSCD.

RESULTS

Expression of WNT16B in the normal human limbus decreases with age

In normal human corneal and limbal tissue, endogenous WNT16B expression was detected mainly throughout the suprabasal and basal layers of the limbal epithelium. Its expression gradually decreased in the superficial layers of the limbal epithelium. By contrast, its expression was very faint in the corneal epithelium (Figure 1A). Similarly, western blotting showed that WNT16B expression was more than 2-fold higher in the limbus than in the central cornea ($p = 0.004$) (Figure 1B). Moreover, mRNA expression of *WNT16B* was 3-fold higher in young donors (0–30 years old) than in middle-aged (30–60 years old, $p = 0.021$) and old (60–90 years old, $p = 0.011$) donors. Similar findings were obtained regarding the mRNA levels of *KI67* ($p = 0.002$ and $p < 0.001$) and *P63α* ($p = 0.102$ and $p < 0.068$) (Figure 1D). The protein expression pattern of WNT16B was consistent with the quantitative real-time PCR findings (Figure 1C), as confirmed by immunofluorescence staining (Figure 1E, $p = 0.090$ and $p < 0.001$) and western blotting (Figure 1F, $p = 0.012$ and $p = 0.002$). The expression level of WNT16B was positively correlated with those of P63, KI67, and K14 but negatively correlated with that of K12 (Figures 1D–1F). These findings indicate that endogenous WNT16B is predominantly expressed in the suprabasal and basal layers of the limbal epithelium, which is generally believed to be the location of LESCs. The expression level of WNT16B decreases with age, which is consistent with age-related reduction of the proliferative capacity of LESCs.

WNT16B enhances proliferation and self-renewal of LECs *in vitro*

To investigate the potential role of WNT16B in proliferation and stemness maintenance of LESCs, cultured LECs were incubated in different concentrations (50, 100, 200, and 400 ng/mL) of exogenous WNT16B. Treatment with 200 or 400 ng/mL WNT16B significantly increased proliferation of LECs, as evidenced by a bigger outgrowth size ($p < 0.001$) and a larger cell number ($p = 0.002$) (Figures 2A–2C). The effect of WNT16B on cell growth in single-cell culture was similar (Figures S1B and S1C). Notably, after the logarithmic growth phase, LECs treated with 200 ng/mL WNT16B retained a more regular morphology than LECs cultured in a control medium (Figure S1D).

To investigate the effect of exogenous WNT16B on stemness maintenance and the proliferative capacity of cultured LECs, the expression levels of the stemness markers of LESC △NP63α and ABCG2, as well as the proliferation marker KI67, were examined. The mRNA expression levels of *△NP63α*, ABCG2, and *KI67* were significantly higher in LECs treated with 200 or 400 ng/mL WNT16B (*△NP63α*: ∼2.5-fold, $p = 0.010$ and $p < 0.001$; ABCG2: ∼3.5-fold, $p = 0.003$ and $p = 0.006$; and *KI67*: ∼5-fold, $p = 0.002$ and $p < 0.001$) than in LECs cultured in a control medium (Figure 2D). Immunofluorescence staining confirmed that treatment with 200 or 400 ng/mL WNT16B significantly increased protein expression of △NP63α ($p = 0.001$ and $p < 0.001$), ABCG2 ($p = 0.002$ and $p = 0.002$), and KI67 ($p = 0.001$ and $p = 0.001$), consistent with the quantitative real-time PCR findings (Figures 2E and 2F).

To further delineate the clonogenic capacity of WNT16B-treated LECs, the colony-formation efficiency (CFE) was evaluated. The CFE increased in a dose-dependent manner following WNT16B treatment and peaked upon treatment with 200 ng/mL WNT16B at an average CFE of 17.1%, which was nearly 3-fold higher than the CFE of LECs cultured in a control medium (6.9%) ($p = 0.010$) (Figure 2G). These findings suggest that exogenous WNT16B enhances proliferation and stemness maintenance of LESCs enriched from limbal culture *in vitro* and that 200 ng/mL is the optimal concentration of exogenous WNT16B for future experiments to investigate the underlying mechanism.

The effects of WNT16B on LECs are mediated by a β-catenin-independent pathway

WNT16 is a ligand for both β-catenin-dependent and -independent signaling pathways, and WNT/β-catenin signaling has been suggested to play a pivotal role in regulating proliferation and stemness maintenance of LESCs. Therefore, we investigated whether the effects of WNT16B (200 mg/mL) on LESCs are regulated by a β-catenin-dependent signaling pathway. Cultured LECs were treated with

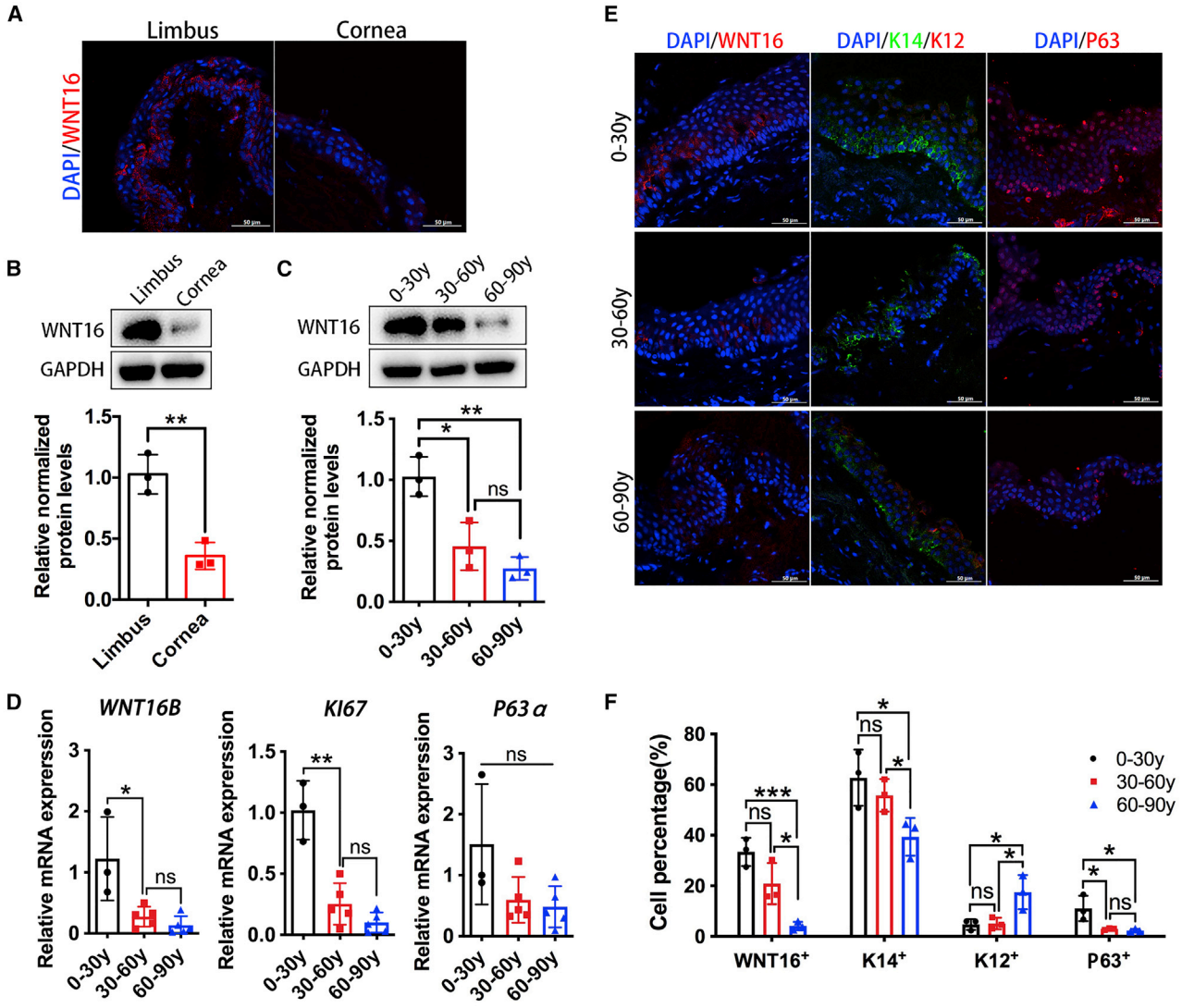

Figure 1. Age-related changes of endogenous WNT16B in the normal human limbus

The normal human cornea and limbus were used to study the localization and age-related changes of endogenous WNT16B.

(A and B) Both immunofluorescence staining (A) and western blotting (B) showed that endogenous WNT16B was mainly expressed in the limbal area ($p = 0.004$), especially in the suprabasal and basal layers of the limbal epithelium. Its expression was not detectable in the corneal epithelium (three independent experiments). To explore age-related changes of WNT16B expression, the corneoscleral rings were divided into three groups according to the age of donors: 0–30 years old ($n = 3$), 30–60 years old ($n = 5$), and 60–90 years old ($n = 5$).

(C–E) Western blotting (C), quantitative real-time PCR (D), and immunofluorescence staining of the limbal epithelium (E) showed that the expression level of WNT16B was significantly higher in the 0–30-year-old group than in the 30–60- and 60–90-year-old groups (western blotting [WB]: $p = 0.016$ and $p = 0.005$, quantitative real-time PCR: $p = 0.021$ and $p = 0.011$, immunofluorescence [IF]: $p = 0.090$ and $p < 0.001$). The mRNA levels of the proliferative marker *KI67* and *P63α* were also measured by quantitative real-time PCR (D). The expression of *KI67* mRNA was significantly higher in the 0–30-year-old group than in the 30–60- and 60–90-year-old groups ($p = 0.002$ and $p < 0.001$).

(E) The age-related reduction of P63 expression in LECs was confirmed by IF staining, and this was accompanied by decreased expression of K14, a biomarker of undifferentiated epithelial cells, and increased expression of K12, a biomarker of differentiated epithelial cells.

(F) Quantitative analysis showed that the percentages of $WNT16B^+$, $K14^+$, and $P63^+$ cells were significantly higher in the 0–30-year-old group than in the 60–90-year-old group ($p < 0.001$, $p = 0.039$, and $p = 0.040$), while the percentage of $K12^+$ cells was significantly higher in the 60–90-year-old group than in the other two groups ($p = 0.036$ and $p = 0.040$). $^*p < 0.05$, $^{**}p < 0.01$, $^{***}p < 0.001$.

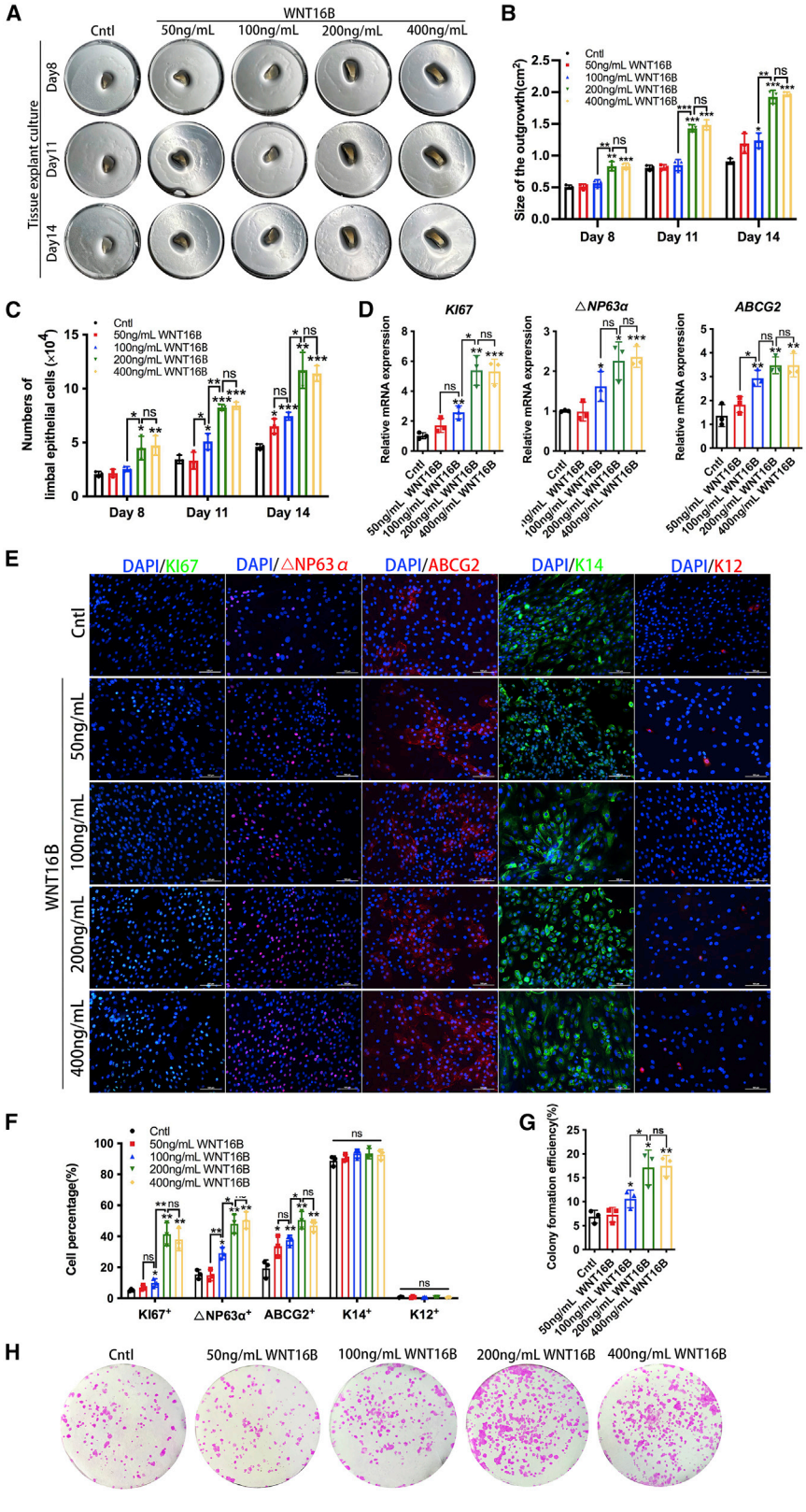

Figure 2. The effect of exogenous WNT16B on the proliferative potential and stemness maintenance of LECs

Primary LECs were treated with different concentrations of exogenous WNT16B *in vitro*, and their proliferative potential and stemness were evaluated. To minimize donor variation, the LECs used in each independent experiment were obtained from the same donor.

(A–C) Quantification of the outgrowth area (A and B) and cell numbers (C) in 24-well showed that the growth of WNT16B-treated LECs was much faster than the growth in the control group, and the effect of WNT16B was dose-dependent and peaked at a concentration of 200 ng/mL (outgrowth: $p^{Day8} = 0.002$, $p^{Day\ 11}$, and $p^{Day14} < 0.001$; cell number: $p^{Day8} = 0.020$, $p^{Day11} < 0.001$, and $p^{Day14} = 0.002$).

(D–F) Quantitative real-time PCR (D), IF staining (E), and quantification of KI67$^+$, △NP63α$^+$, ABCG2$^+$, K14$^+$, and K12$^+$ cells (F) showed that WNT16B treatment increased the expression levels of KI67, △NP63α, and ABCG2. These effects were dose-dependent and peaked at a concentration of 200 ng/mL (KI67: p = 0.002 and p = 0.001; △NP63α: p = 0.010 and 0.001; and ABCG2: p = 0.003 and 0.002) and plateaued at concentrations higher than 200 ng/mL. The expression of neither K14 nor K12 was affected by exogenous WNT16B (E and F).

(G and H) The capacity of WNT16B to promote proliferation of LECs was also evaluated by determining the CFE. The clonogenic capacity of LECs was significantly enhanced by WNT16B treatment and peaked at concentration of 200 ng/mL (p = 0.010). The effects of 200 and 400 ng/mL WNT16B on cell outgrowth, proliferation, and the expression of stemness biomarkers of LECs did not show any significant differences, indicating that the stimulatory effect of WNT16B plateaued at concentrations higher than 200 ng/mL. Data are from three independent experiments. *p < 0.05, **p < 0.01, ***p < 0.001.

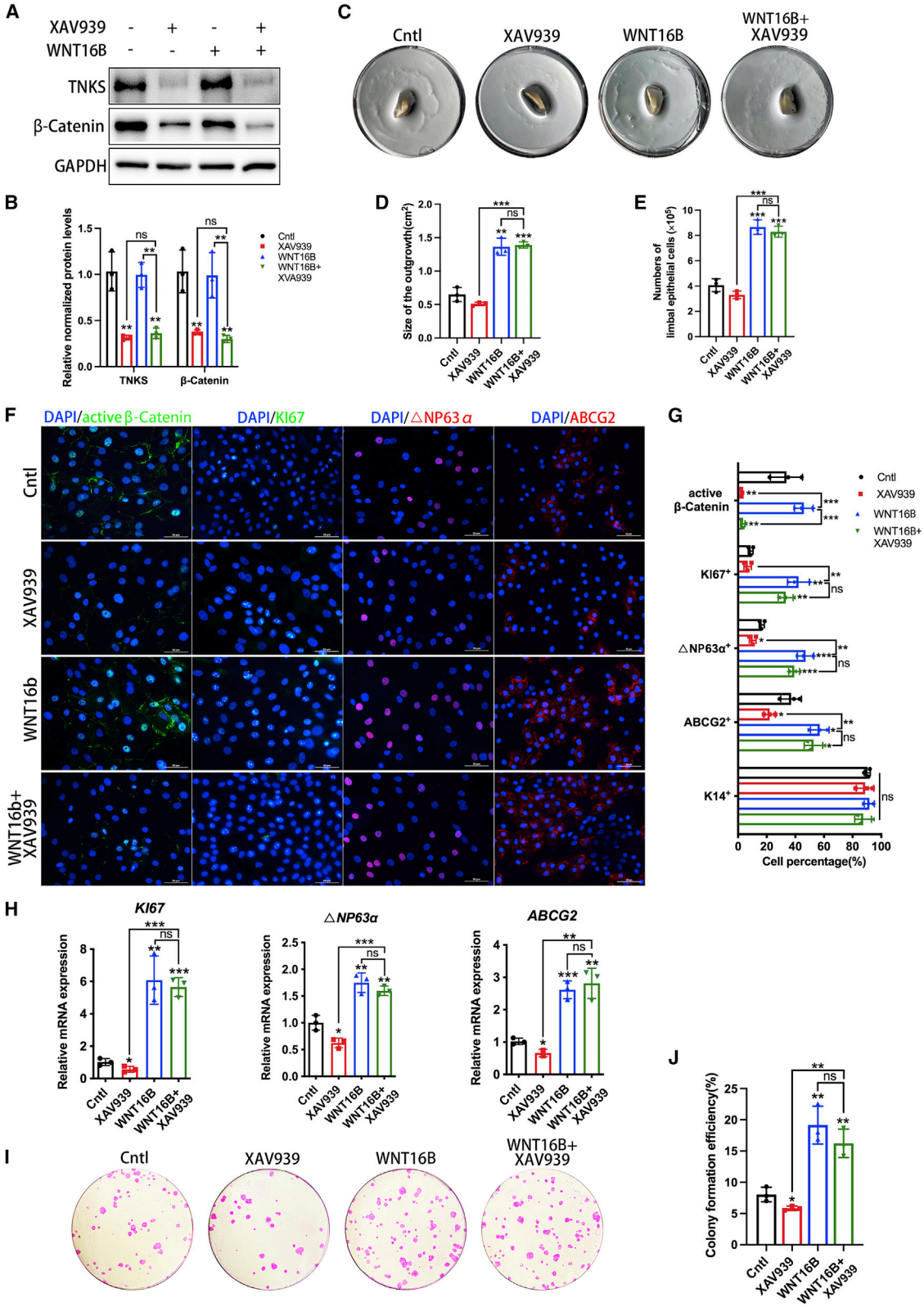

(legend on next page)

the small molecule XAV939 (10 μmol/L, from D0) (Figure S1E), which selectively inhibits the WNT/β-catenin signaling pathway by suppressing tankyrase (TNKS) and stimulating phosphorylation of cytosolic β-catenin (Huang et al., 2009). The treatment of either XAV939 alone or WNT16B + XAV939 significantly reduced the protein levels of TNKS ($p = 0.004$ and $p = 0.006$) and β-catenin ($p = 0.008$ and $p = 0.006$) in LESCs (Figures 3A and 3B). The extent of cell outgrowth and cell numbers of LECs treated with WNT16B + XAV939 were significantly larger than those in the control group (both $p < 0.001$) and were similar to those of LECs treated with WNT16B only (Figures 3C–3E). Immunofluorescence staining showed that exogenous WNT16B failed to activate cytosolic β-catenin and induce nuclear translocation of β-catenin (Figure 3F). Moreover, XAV939 treatment reduced the expression of active nuclear β-catenin in LECs, regardless of whether they were cultured in a control medium or treated with WNT16B ($p = 0.008$ and $p = 0.010$). However, the comparisons on the protein (Figures 3F and 3G) and mRNA (Figure 3H) levels of *KI67*, *△NP63α*, and ABCG2 did not show any significant differences between LECs co-treated with WNT16B + XAV939 and LECs treated with WNT16B only (Figures 3F–3H). The clonogenic capacity of LECs treated with WNT16B + XAV939 was similar to that of LECs treated with WNT16B only. These results indicate that the inhibition of β-catenin does not affect the proliferation capacity and stemness of LESCs. The effects of WNT16B on LECs enriched for LESCs are mediated via a β-catenin-independent pathway.

The effects of WNT16B on LECs are mediated by the CXCR4/MEK/ERK signaling pathway

To further investigate the molecular mechanism underlying the effects of WNT16B on LESCs, RNA sequencing was performed to identify genes whose expression changed in response to exogenous WNT16B. Compared with LECs cultured in a control medium, transcriptomics approaches with edgeR identified 445 genes (Table S3) that were differentially expressed in WNT16B-treated LECs with a false discovery rate (FDR) ≤ 0.05 and $|\log2FC| \geq 1$. In total, 262 upregulated mRNAs and 183 downregulated mRNAs were identified (Figure 4A). GOATOOLS was used to analyze the enriched Gene Ontology (GO) terms with FDR ≤ 0.05. According to the rich factors, the most enriched terms were associated with binding of receptors and ligands. According to the gene numbers, the most enriched terms were involved in the developmental process (Figure 4B). KOBAS was used to perform KEGG pathway analysis of differentially expressed genes (DEGs) with FDR ≤ 0.05. "Cytokine-cytokine receptor interaction" was the leading enriched KEGG pathway (Figure 4C). Among the top ten DEGs in response to exogenous WNT16B treatment (Figure 4D), C-X-C chemokine receptor type 4 (*CXCR4*) ($|\log2FC| = 5.32$) is a vital element of cytokine-cytokine receptor interaction pathways. It is predominantly expressed in the limbus and is involved in stemness maintenance of LESCs (Xie et al., 2011). Therefore, we considered *CXCR4* to be the key factor that responds to WNT16B and plays a crucial role in mediating the effects of WNT16B on cultured LECs.

To validate the differential expression of *CXCR4* identified by RNA sequencing, quantitative real-time PCR was performed. This confirmed that *CXCR4* expression was 2.4-fold higher in WNT16B-treated LECs than in control LECs ($p = 0.045$) (Figure 5A). CXCR4 is believed to be important in many cell biological processes and to activate a series of downstream signals including the MEK-ERK, JAK-STAT, and PI3K-AKT signaling pathways. Therefore, we measured the protein levels of key elements in these three signaling pathways. The phosphorylation levels of MEK and ERK were ~2- ($p = 0.024$) and ~2.5-fold ($p = 0.002$) higher in WNT16B-treated LECs than in control LECs, respectively, in accordance with the increased expression of CXCR4 ($p < 0.001$). However, the phosphorylation levels of STAT and AKT did not significantly differ between WNT16B-treated and control LECs (Figures 5B

Figure 3. The role of the canonical β-catenin signaling pathway in the effects of exogenous WNT16B on LECs

(A and B) WB showed that the protein level of TNKS and β-catenin in LECs was unchanged with the treatment of exogenous WNT16B but was significantly inhibited by the treatment of either 10 μmol/L XAV939 ($p = 0.004$ and $p = 0.008$) or WNT16B + XAV939 (both $p = 0.006$). However, no significant differences were found between these two interventions.

(C–E) Quantification of the outgrowth area (C and D) and cell numbers € on the [1]1th day showed that the growth of WNT16B + XAV939 co-treated LECs was much faster than those of the control and XAV939-treated LECs (both $p < 0.001$) but was similar to those of WNT16B-treated LECs.

(F and G) IF staining (F) and quantification of cells expressing active β-catenin, KI67, △NP63α, and ABCG2 (G) showed that although active nuclear β-catenin was significantly inhibited in LECs co-treated with XAV939 + WNT16B ($p = 0.010$), expression of KI67, △NP63α, and ABCG2 did not significantly differ between these cells and LECs treated with WNT16B only.

(H) Quantitative real-time PCR revealed that the mRNA expression profiles of *KI67*, *△NP63α*, and ABCG2 were almost the same in LECs co-treated with XAV939 + WNT16B and LECs treated with WNT16B only.

(I and J) The clonogenic capacity of WNT16B + XAV939 co-treated LECs was significantly stronger than that of control and XAV939-treated LECs ($p = 0.005$ and $p = 0.002$) but was similar to that of WNT16B-treated LECs. Data are from three independent experiments. *$p < 0.05$, **$p < 0.01$, ***$p < 0.001$.

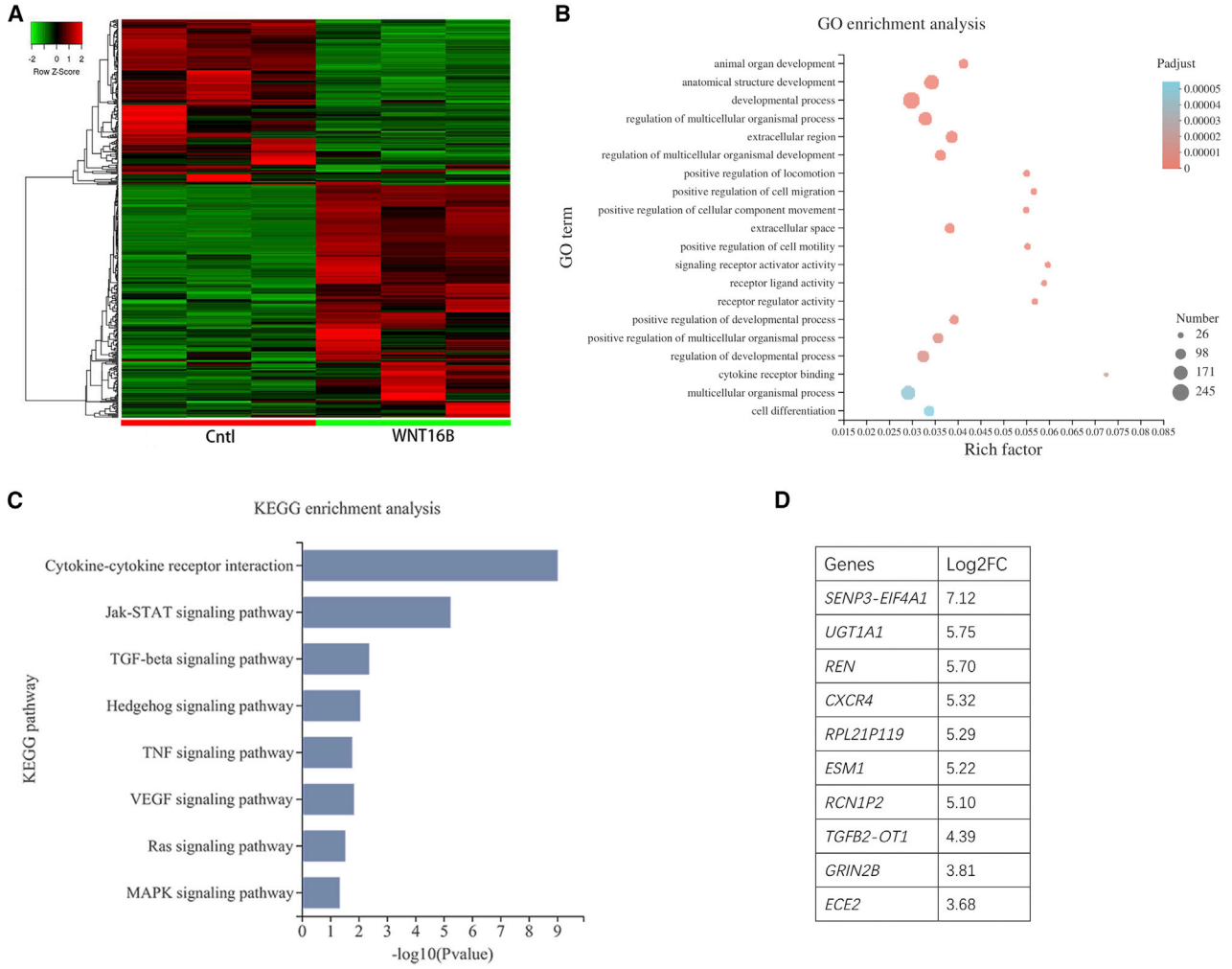

Genes	Log2FC
SENP3-EIF4A1	7.12
UGT1A1	5.75
REN	5.70
CXCR4	5.32
RPL21P119	5.29
ESM1	5.22
RCN1P2	5.10
TGFB2-OT1	4.39
GRIN2B	3.81
ECE2	3.68

Figure 4. RNA sequencing analysis and determination of the top DEGs

(A) A total of 445 DEGs between control and WNT16B-treated LECs were identified, as shown by the heatmap.

(B and C) GO (B) and KEGG (C) enrichment analyses of these 445 DEGs showed that the leading highly enriched KEGG pathways were those involved in environmental information processing (cytokine-cytokine receptor interaction, JAK-STAT signaling, and Hedgehog signaling) and the organismal system (interleukin [IL]-17 signaling pathways).

(D) Among them, the top ten DEGs in terms of Log2FC are listed.

and 5C). These results indicate that WNT16B activates the CXCR4/MEK/ERK signaling pathway.

Next, to determine whether MEK/ERK signaling activated by CXCR4 is involved in the enhanced proliferation and self-renewal of WNT16B-treated LESCs, a specific CXCR4 antagonist, AMD3100 (Fricker et al., 2006) (20 μg/mL, from D0) (Figure S1F), was used in the culture system. Western blotting showed that CXCR4 expression was significantly lower in LECs co-treated with WNT16B + AMD3100 than in LECs treated with WNT16B only ($p < 0.001$) (Figures 5D and 5E). The involvement of MEK/ERK signaling was also verified by western blotting, which showed significantly lower phosphorylation levels of MEK ($p = 0.015$) and ERK ($p = 0.010$) in LECs co-treated with AMD3100 + WNT16B than in LECs treated with WNT16B only (Figures 5D and 5E).

The outgrowths and cell numbers showed that the increased growth of WNT16B-treated LECs was significantly inhibited by AMD3100 ($p = 0.005$ and $p = 0.002$) (Figures 5F–5H). The mRNA and protein levels of *KI67* ($p < 0.003$ and $p = 0.049$), $\Delta NP63\alpha$ ($p = 0.006$ and $p = 0.003$), and ABCG2 ($p = 0.034$ and $p = 0.014$) were lower in LECs co-treated with WNT16B + AMD3100 than in LECs treated with WNT16B only (Figures 5I–5K). Accordingly, the clonogenic capacity of LECs co-treated with WNT16B + AMD3100 was significantly weaker than that

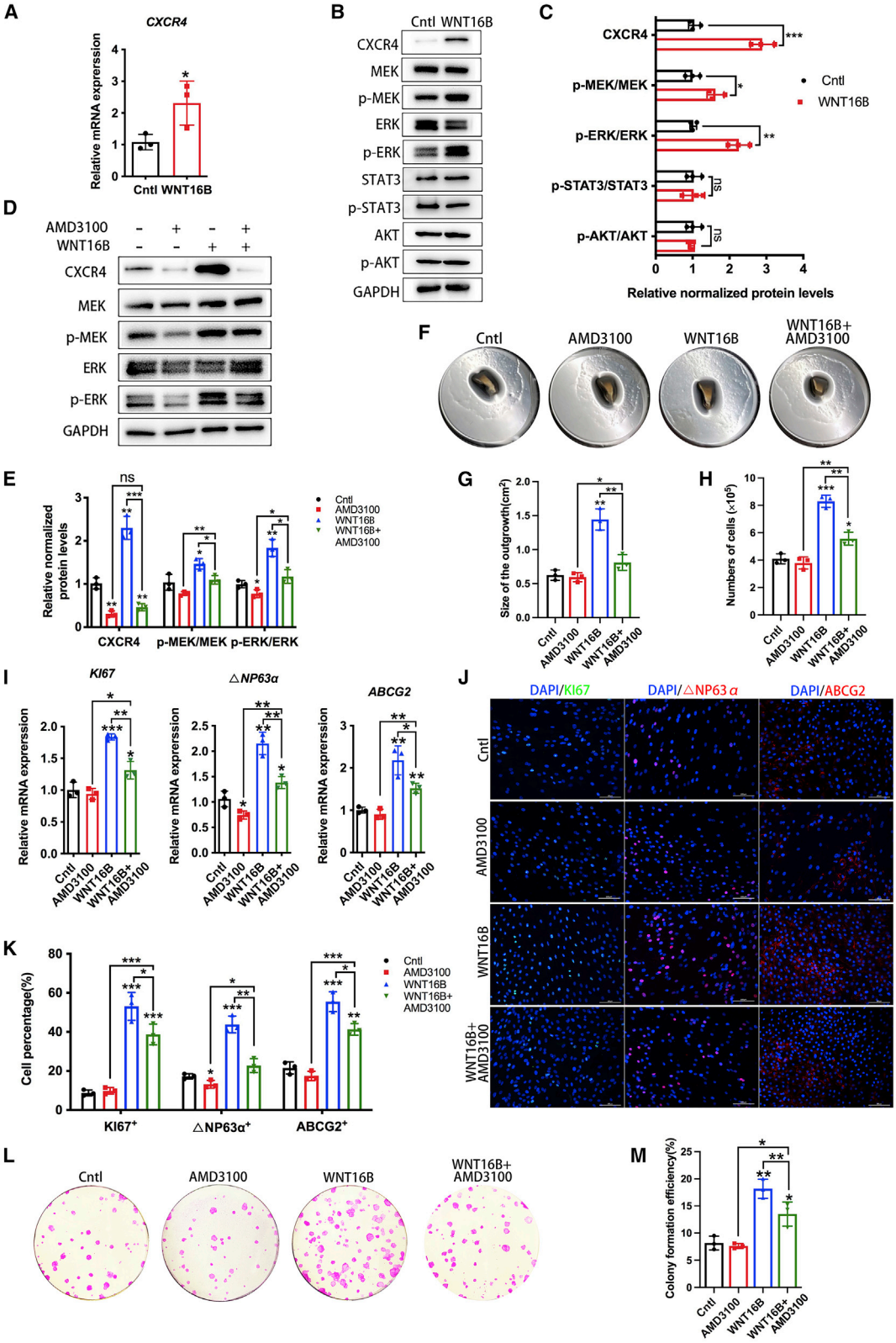

(legend on next page)

of LECs treated with WNT16B only ($p = 0.046$). AMD3100 alone did not affect the clonogenic capacity of LECs (Figures 5L and 5M). These results indicate that the stimulatory effects of WNT16B on self-renewal and the proliferative potential of LECs were abolished by inhibition of CXCR4. Together, these findings confirm that WNT16B enhances proliferation and self-renewal of LECs by activating the CXCR4/MEK/ERK signaling pathway.

WNT16B accelerates corneal-epithelial wound healing and enhances the proliferation of LESCs *in vivo*

Three WNT16B-targeting, cholesterol-modified small interfering RNAs (siRNAs) (si*Wnt16b*s) were designed to block the effects of endogenous WNT16B, and their knockdown efficiencies were evaluated by quantitative real-time PCR (Figure 6A) and western blotting (Figure 6B). It turned out that they significantly blocked expression of endogenous *Wnt16b* at both mRNA and protein levels (*siWnt16b*-1: $p = 0.004$; si*Wnt16b*-2: $p < 0.001$; and si*Wnt16b*-3: $p < 0.001$). The knockdown efficiency of si*Wnt16b*-3 was higher than those of si*Wnt16b*-1 and si*Wnt16b*-2; therefore, si*Wnt16b*-3 was used in further experiments.

A mouse model of corneal-epithelial wound healing was established to investigate the potential of WNT16B to repair corneal-epithelial injury. The mice were divided into the following four groups: control group (tobramycin eye drops), WNT16B group (exogenous WNT16B eye drops plus tobramycin eye drops), si*Wnt16b* group (transfection of si*Wnt16b*-3 plus tobramycin eye drops), and siControl group (transfection of scrambled siRNA plus tobramycin eye drops). Fluorescein staining under a slit-lamp biomicroscope showed that the areas of epithelial defects were significantly smaller in the WNT16B group than in the other three groups at 12 and 24 h (control: $p = 0.016$ and $p < 0.001$, si*Wnt16b*: $p = 0.007$ and $p < 0.001$, and siControl: $p = 0.013$ and $p < 0.001$). Epithelial defects were completely healed in the WNT16B group at 48 h. By contrast, the areas of epithelial defects were significantly larger in the si*Wnt16b* group than in the siControl group at 24 and 48 h (all $p < 0.001$) (Figures 5C and 5D). These findings indicate that WNT16B accelerates repair of the corneal epithelium after injury.

To evaluate the effect of WNT16B on LESCs *in vivo*, expression of P63 and ABCG2 was assessed at 48 h after corneal-epithelial wound healing. Immunofluorescence staining showed that the number of $P63^+$ and $ABCG2^+$ cells was significantly higher in the WNT16B group than in the control group ($p = 0.009$ and $p = 0.038$), and the expression of P63 was significantly lower in the si*Wnt16b* group than in the siControl group ($p = 0.007$) (Figures 6E and 6F). These results indicate that WNT16B enhances the proliferation of LECs *in vivo*.

DISCUSSION

WNT signaling plays an important role in homeostasis maintenance of LESCs (González et al., 2019; Lee et al., 2017; Nakatsu et al., 2011; Zheng et al., 2019), and canonical WNT/β-catenin signaling is mainly involved in this function (González et al., 2019; Nakatsu et al., 2011; Ouyang et al., 2014). WNT16B reportedly participates in proliferation and stemness maintenance of many types of adult stem cells via canonical or non-canonical WNT signaling pathways (Mendoza-Reinoso and Beverdam, 2018; Meyers et al., 2018; Ozeki et al., 2016; Teh et al., 2007). Our study revealed that treatment with a selective β-catenin inhibitor did not block WNT16B-induced cell proliferation and did not affect the expression levels of a proliferation marker (KI67) and stemness markers ($\triangle NP63\alpha$ and ABCG2). This demonstrates that the effects of WNT16B on LECs enriched for LESCs are β-catenin-independent. Our study is the first to report the mechanism of WNT16B in homeostasis maintenance of human LESCs.

Figure 5. The mechanism by which WNT16B enhances proliferation and self-renewal of LECs via the CXCR4 signaling pathway

(A) Quantitative real-time PCR confirmed that the mRNA level of *CXCR4* was significantly higher in WNT16B-treated LECs than in control LECs ($p = 0.045$).

(B and C) WB showed that in addition to an increased level of CXCR4, the phosphorylation levels of MEK and ERK were significantly increased by WNT16B treatment ($p = 0.024$ and $p = 0.002$). However, the phosphorylation levels of STAT3 and AKT were not changed.

(D) WB showed that AMD3100 treatment inhibited CXCR4 expression no matter whether LECs were untreated ($p = 0.001$) or WNT16bB-treated ($p < 0.001$). The phosphorylation levels of MEK and ERK were significantly lower in LECs co-treated with AMD3100 + WNT16B than in LECs treated with WNT16B only ($p = 0.015$ and $p = 0.010$).

(F–H) Quantification of outgrowth area (F and G) and cell numbers (H) on the 11th day of LECs treated with WNT16B + AMD3100 were significant smaller than LECs treated with WNT16B only ($p = 0.005$ and $p = 0.002$).

(I–K) Moreover, quantitative real-time PCR (I), IF staining (J), and quantification of $KI67^+$, $\triangle NP63\alpha^+$, and $ABCG2^+$ cells (K) showed that the enhanced levels of KI67, $\triangle NP63\alpha$, and ABCG2 induced by WNT16B treatment were significantly decreased by AMD3100 treatment (KI67: $p = 0.001$ and 0.049; $\triangle NP63\alpha$: $p = 0.006$ and 0.003; and ABCG2: $p = 0.034$ and 0.014).

(L and M) Studies of CFE showed that the clonogenic capacity of LECs co-treated with WNT16B + AMD3100 was significantly lower than that of LECs treated with WNT16B only ($p = 0.046$). AMD3100 alone did not affect the clonogenic capacity of LECs. Data are from three independent experiments. *$p < 0.05$, **$p < 0.01$, ***$p < 0.001$.

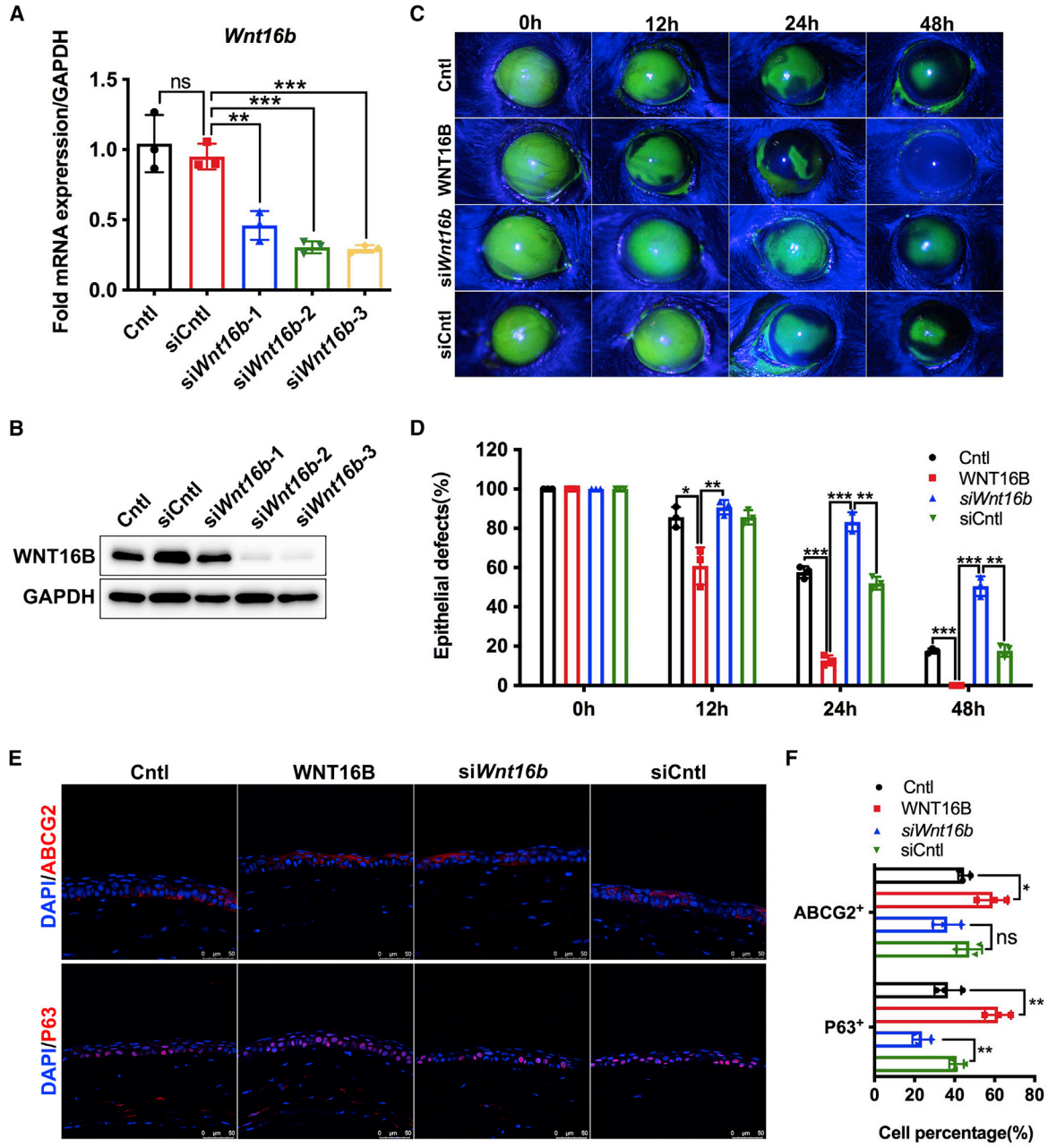

Figure 6. The functional role of WNT16B in mouse corneal-epithelial wound healing

Cholesterol-modified siRNAs specific to WNT16B (si*Wnt16b*s) or scrambled siRNA (siControl) were subconjunctivally injected, and mouse limbal tissues were obtained 24 h after injection to verify the knockdown efficiencies of si*Wnt16b*s.

(A and B) Quantitative real-time PCR (A) and WB (B) showed that the knockdown efficiency of si*Wnt16b*-3 was higher than those of the other two siRNAs, and thus si*Wnt16b*-3 was used in further experiments (three independent experiments).

(C) After completely removing the corneal epithelium of mice (n = 12), healing of corneal-epithelial defects was evaluated by fluorescein staining at 0, 12, 24, and 48 h.

(D) Quantification of the epithelial defect area showed that the epithelium healed significantly faster in the WNT16B group (n = 3) than in the control (n = 3) and si*Wnt16b* (n = 3) groups based on measurements at 12, 24, and 48 h (control: $p = 0.016$, $p < 0.001$, and $p < 0.001$ and si*Wnt16b*: $p = 0.007$, $p < 0.001$, and $p < 0.001$). Moreover, epithelial defects were significantly larger in the si*Wnt16b* group than in the siControl group (n = 3) at 24 and 48 h (both $p < 0.001$).

(legend continued on next page)

CXCR4, one of the most widely expressed chemokine receptors, was found to respond to WNT16B. CXCR4 is generally considered to participate in cell proliferation, stem-cell activation, and tissue regeneration by binding to its ligand SDF-1 and activating multiple signaling pathways including the MEK/ERK, PI-3K/AKT, JAK/STAT, and mTOR signaling pathways. In normal human eyes, CXCR4 is preferentially expressed in $P63^+$ LECs and stromal cells and maintains homeostasis and self-renewal of LESCs through the SDF-1/CXCR4 signaling pathway (Albert et al., 2012; Xie et al., 2011). CXCR4 is also reported to mediate TFF3-induced migration of corneal epithelial cells (Dieckow et al., 2016) and to function in corneal neovascularization and lymphangiogenesis (Du and Liu, 2016). The relationship between CXCR4 and WNT signaling has been reported in fibroblasts and vascular endothelial cells (He et al., 2019; Song et al., 2018). The current study demonstrated that CXCR4 activates MEK/ERK signaling in response to WNT16B. Activated MEK/ERK signaling plays a pivotal role in the proliferation of corneal epithelial cells and many other cell types/cancer cells (Coutant et al., 2002; Lee and Kay, 2011; Shen et al., 2010; Wang et al., 2018, 2019). Inhibition of CXCR4 significantly decreased the levels of *p*-MEK1/2, *p*-ERK1/2, KI67, $\triangle$NP63α, and ABCG2 in LESCs but did not affect the levels of p-STAT3 and *p*-AKT. These results suggest that WNT16B enhances proliferation and stemness maintenance of LECs by activating the CXCR4/MEK/ERK signaling cascade. Further research is needed to elucidate the molecular mechanism underlying the relationship between WNT16B and CXCR4.

The proliferation potential and stemness of several types of stem cells, including mesenchymal stem cells, neural stem cells, and LESCs, reportedly decrease with age (Bouab et al., 2011; Zaim et al., 2012; Zheng and Xu, 2008). The current study confirmed that expression of P63, K14, and KI67 decreased with age in normal human limbal tissue, consistent with previous reports (Arpitha et al., 2005; Eghtedari et al., 2016; Gerdes et al., 1983). Moreover, expression of endogenous WNT16B also declined with age, indicating that younger donors potentially had more functional LESCs with greater proliferative capacities and higher expressions of WNT16B. Comparisons of the proliferative and self-renewal capacities of *in-vitro*-cultured LECs from young donors and old ones are needed in further studies to verify these *in-vivo* findings. It is notable that WNT16B enhanced proliferation and stemness maintenance of LESCs, and the treatment with exogenous WNT16B remarkably accelerated corneal-epithelial wound healing in mice. It is challenging to maintain the self-renewal ability of LESCs during expansion *in vitro*. WNT16B might be a useful tool to optimize the culture conditions of LECs enriched for LESC and improve the quality of cultured cell sheets.

EXPERIMENTAL PROCEDURES

Primary LEC culture

Cadaveric human corneoscleral tissues were obtained from an eye bank with the approval of the Ethics Committee of the Eye, Ear, Nose and Throat Hospital of Fudan University. Corneoscleral tissues that did not meet the criteria for clinical use and were stored in Optisol at 4°C for fewer than 5 days were used for cell culture. The tissues were washed thrice in cold phosphate-buffered saline (PBS) containing 100 U/mL penicillin, 100 U/mL streptomycin, and 1.25 μg/mL amphotericin B. Excessive sclera, conjunctiva, iris, trabecular meshwork, and endothelium were carefully removed.

Two culture systems were used in this study. In the tissue-explant culture system, corneoscleral rims including a 1-mm-wide peripheral cornea and 1-mm-wide sclera were cut into 2 × 2-mm pieces, which were then placed on culture plates with the epithelial sides facing down. The culture medium was DMEM/F12 (Gibco) containing 1% penicillin-streptomycin (Gibco), 10% fetal bovine serum (Gibco), 10 ng/mL EGF (Sigma-Aldrich), 5 μg/mL insulin (MedChemExpress), 1% N-2 (Gibco), and 0.5% dimethyl sulfoxide (Sigma-Aldrich). Cultures were incubated at 37°C in 5% CO_2 for 11–14 days, and the growth medium was refreshed every 2–3 days. In the single-cell culture system, corneoscleral rims were cut into small segments and incubated with 2.4 U/mL Dispase II (Roche) at 37°C for 2 h. The limbal epithelium was carefully peeled away under a dissecting microscope and treated with 0.25% trypsin-EDTA at 37°C for 5 min to obtain a single-cell suspension. The cell suspensions were seeded at a density of 200 cells/cm^2 on a growth-arrested NIH-3T3 feeder cell layer (3×10^4 cells/cm^2, Cell Bank of the Chinese Academy of Sciences), which was pretreated with 4 μg/mL mitomycin C (MedChemExpress) at 37°C for 2 h. The culture medium and culture conditions were exactly the same as those used in the tissue-explant culture system. The identification of cell phenotype is shown in Figure S1A.

Evaluation of cell growth

The images of the outgrowth of tissue-explant culture were captured on the 8th, 11th, and 14th days. The cell morphology and outgrowth areas of cultured LECs were captured using an inverted microscope. The outgrowth area was measured with the software ImageJ (National Institutes of Health, USA, https://imagej.nih.gov/ij/) and quantified using the following formula: size of cell outgrowth = (outgrowth area - tissue area)/well area × 2 cm^2. The cultured cells were harvested at the above time points to count total cell numbers.

(E and F) Immunofluorescence staining (E) and quantification of $P63^+$ and $ABCG2^+$ cells (F) showed that P63 and ABCG2 expression was higher in the WNT16B group than in the control group ($p = 0.009$ and $p = 0.038$). Expression of P63 was significantly lower in the si*Wnt16b* group than in the siControl group ($p = 0.007$), whereas expression of ABCG2 was similar in these two groups ($p = 0.117$). *$p < 0.05$, **$p < 0.01$, ***$p < 0.001$.

Quantitative real-time PCR

Total RNA was extracted using an RNAsimple Total RNA Kit (Tiangen) and then reverse transcribed with FastKing gDNA Dispelling RT Super-Mix (Tiangen). Quantitative real-time PCR assays were performed using a QuantiNova SYBR Green PCR Kit (Qiagen) and ViiA7 Real-time PCR System (Applied Biosystems). The conditions were 2 min of initial activation at 95°C, followed by 40 cycles of 5 s of denaturation at 95°C and 20 s of annealing and extension at 60°C. The ΔΔCT method was used to calculate relative mRNA fold changes. Three replications were performed, and data are shown as mean ± SD. Primer information is provided in Table S1.

Immunofluorescence staining

Human corneoscleral tissues were fixed in 4% paraformaldehyde (Beyotime Biotechnology) for 20 min, dehydrated in graded sucrose, embedded in an optimum-cutting-temperature compound (SAKURA), and preserved at -80°C. The embedded tissue was cut into 10-μm-thick sections with a freezing microtome (Leica). For immunofluorescence staining, cultured cells were seeded on coverslips and fixed with 4% paraformaldehyde for 20 min. Sections and paraformaldehyde-fixed LECs were permeabilized with PBS (Songon Biotech) containing 0.3% Triton X-100 (Sigma-Aldrich) for 10 min, blocked with PBS containing 3% BSA (BSA, Roche) for 1 h at room temperature, and incubated with primary antibodies diluted in 1% BSA and 0.1% Triton X-100 overnight at 4°C. Thereafter, the sections and cells were washed thrice in PBS, incubated with secondary antibodies for 1 h at room temperature, and then washed thrice in PBS. Nuclei were labeled with 4′,6-diamidino-2-phenylindole (DAPI; Invitrogen) for 5 min at room temperature, and then samples were washed thrice in PBS and mounted in 50% glycerinum (Sigma-Aldrich). Images were acquired using a Leica TCS SP8 confocal microscope and a Leica DM4000B fluorescence microscope. Fluorescent signals in three randomly selected areas were quantified using ImageJ software (National Institutes of Health, USA). Antibody information is provided in Table S2.

Western blotting

Cells were washed once in PBS, lysed with radioimmunoprecipitation assay (RIPA) lysis buffer (Beyotime Biotechnology) supplemented with a protease and phosphatase inhibitor cocktail (Beyotime Biotechnology), and centrifuged to obtain a supernatant. The protein concentration was quantified using an Enhanced BCA Protein Assay Kit (Beyotime Biotechnology). Proteins were separated by 10% SDS-polyacrylamide gel electrophoresis (EpiZyme) and transferred to a polyvinylidene fluoride membrane (Millipore) according to standard protocols. The membranes were blocked with TBST (Songon Biotech) containing 5% fat-free milk and incubated with specific primary antibodies overnight at 4°C. After three washes with TBST, the membranes were incubated with secondary antibodies for 1 h at room temperature. Glyceraldehyde 3-phosphate dehydrogenase (GAPDH) served as the loading control. Antibody information is provided in Table S2.

CFE assay

Isolated LECs were seeded at a density of 1×10^3 cells/well on an NIH-3T3 feeder-cell layer in 6-well plates. After 14 days of culture, epithelial clones were fixed with 4% paraformaldehyde for 20 min and stained with 0.5% rhodamine B (RHAWN) for 15 min at room temperature. The CFE was calculated by dividing the number of colonies by the number of seeded LECs.

RNA sequencing analysis

Total RNA was extracted using TRIzol reagent (Invitrogen), and genomic DNA was removed using DNaseI (TaKara). The RNA quality was determined using a 2100 Bioanalyser (Agilent), and RNA was quantified using an ND-2000 spectrophotometer (NanoDrop Technologies). Only high-quality RNA samples (OD260/280 = 1.8–2.2, OD260/230 ≥ 2.0, RIN ≥ 6.5, 28S:18S ≥ 1.0, and >1 μg) were used to construct sequencing libraries. A total of 1 μg RNA was used to prepare an RNA-sequencing transcriptome library using a TruSeq RNA Sample Preparation Kit (Illumina). Briefly, mRNA was isolated according to the polyA selection method using oligo (dT) beads and converted to cDNA using a SuperScript Double-Stranded cDNA Synthesis Kit (Invitrogen) with random hexamer primers (Illumina). Thereafter, the synthesized cDNA was subjected to end-repair, phosphorylation, and "A" base addition according to Illumina's library-construction protocol. Libraries were size selected for cDNA target fragments of 300 bp using 2% Low Range Ultra Agarose followed by PCR amplification using Phusion DNA polymerase (NEB) for 15 cycles. After quantification using a TBS380 fluorometer, the paired-end RNA sequencing library was sequenced with an Illumina HiSeq X Ten/NovaSeq 6000 sequencer (2 × 150 bp read length).

Differential expression analysis was performed using edgeR with a Q value ≤0.05. Genes with |log2FC| > 1 and a Q value ≤0.05 were considered to be significantly differentially expressed. Functional enrichment analyses including GO and KEGG were performed to identify which DEGs were significantly enriched in GO terms and metabolic pathways with a Bonferroni-corrected p value of ≤0.05 in comparison with the whole transcriptome. GO functional enrichment and KEGG pathway analyses were performed using GOATOOLS (https://github.com/tanghaibao/Goatools) and KOBAS (http://kobas.cbi.pku.edu.cn/home.do).

Corneal-epithelial wound-healing model

The animal studies were approved by the Animal Experiment Ethics Committee of the Eye, Ear, Nose and Throat Hospital of Fudan University and were performed in accordance with the statement of the Association for Research in Vision and Ophthalmology (ARVO) entitled "Use of Animals in Ophthalmic and Vision Research."

C57BL/6 mice (6–8 weeks old, male) were anesthetized with an intraperitoneal injection of 4% chloral hydrate (0.1 mL/10 g). To establish a corneal-epithelial wounding model, the central corneal epithelium was demarcated using a 2.5-mm-diameter trephine and was scraped thoroughly under an operating microscope. The experimental group was topically treated with recombinant WNT16B solution (200 ng/mL) and tobramycin eye drops (Alcon) thrice per day, while the control group was treated only with tobramycin eye drops. Another two groups were used to determine the effect of endogenous WNT16B on epithelium healing. Cholesterol-modified si*Wnt16b*s (LncBio) were used to knock down endogenous WNT16B expression in mice by transient transfection. Three si*Wnt16b*s and a scrambled siRNA (siControl) were

diluted to a concentration of 50 nM, and 5 μL was subconjunctivally injected using a Hamilton syringe at 24 h before epithelium scraping. The knockdown efficiency was evaluated, and the most efficient si*Wnt16b* was selected for further experiments. Mice injected with si*Wnt16b* or siControl were treated with regular tobramycin eye drops thrice per day. Corneal fluorescein staining was used to observe the defect area of the corneal epithelium and recorded by slit-lamp photography. A histogram of epithelial defects was presented as the percentages of the original wound size using ImageJ software.

Statistical analysis

Statistical analyses were performed using GraphPad Prism 8 software (USA). All data were presented as the mean ± SD Groups were compared using the two-tailed unpaired t test and a one-way analysis of variance. A p value <0.05 was considered statistically significant.

Data and code availability

All data supporting the findings of this study are available within the paper and its supplementary information file. The accession number for the sequence data reported in this paper is GEO: GSE180698.

SUPPLEMENTAL INFORMATION

Supplemental information can be found online at https://doi.org/10.1016/j.stemcr.2022.03.001.

AUTHOR CONTRIBUTIONS

Conceptualization, Q.L., L.G., and S.Z.; methodology, Q.L., S.Z., and Y.D.; investigation, S.Z., Y.D., and X.W.; writing – original draft, S.Z; writing – review & editing, S.Z. and Q.L.; funding acquisition, Q.L. and L.G.; supervision, Q.L. and L.G. All authors read and approved the final manuscript.

CONFLICTS OF INTEREST

The authors declare no competing interests.

ACKNOWLEDGMENTS

The authors thank Jianjiang Xu, Jun Xiang, Tingyan Gong, and Jiayu Gu for their support with donor tissue acquisition and collection, as well as Shuoer Wang for technical guidance. This work was supported by the Natural Science Foundation of China (NSFC) (81970767 and 82070924) and the Natural Science Foundation of Shanghai (SCST) (19ZR1408200).

Received: July 30, 2021
Revised: March 1, 2022
Accepted: March 2, 2022
Published: March 31, 2022

REFERENCES

Albert, R., Veréb, Z., Csomós, K., Moe, M.C., Johnsen, E.O., Olstad, O.K., Nicolaissen, B., Rajnavölgyi, E., Fésüs, L., Berta, A., and Petrovski, G. (2012). Cultivation and characterization of cornea limbal epithelial stem cells on lens capsule in animal material-free medium. PloS One *7*, e47187. https://doi.org/10.1371/journal.pone.0047187.

Arpitha, P., Prajna, N.V., Srinivasan, M., and Muthukkaruppan, V. (2005). High expression of p63 combined with a large N/C ratio defines a subset of human limbal epithelial cells: implications on epithelial stem cells. Invest. Ophthalmol. Vis. Sci. *46*, 3631–3636. https://doi.org/10.1167/iovs.05-0343.

Bouab, M., Paliouras, G.N., Aumont, A., Forest-Bérard, K., and Fernandes, K.J. (2011). Aging of the subventricular zone neural stem cell niche: evidence for quiescence-associated changes between early and mid-adulthood. Neuroscience *173*, 135–149. https://doi.org/10.1016/j.neuroscience.2010.11.032.

Clevers, H., Loh, K.M., and Nusse, R. (2014). Stem cell signaling. an integral program for tissue renewal and regeneration: Wnt signaling and stem cell control. Science *346*, 1248012. https://doi.org/10.1126/science.1248012.

Coutant, A., Rescan, C., Gilot, D., Loyer, P., Guguen-Guillouzo, C., and Baffet, G. (2002). PI3K-FRAP/mTOR pathway is critical for hepatocyte proliferation whereas MEK/ERK supports both proliferation and survival. Hepatology *36*, 1079–1088. https://doi.org/10.1053/jhep.2002.36160.

Dieckow, J., Brandt, W., Hattermann, K., Schob, S., Schulze, U., Mentlein, R., Ackermann, P., Sel, S., and Paulsen, F.P. (2016). CXCR4 and CXCR7 mediate TFF3-induced cell migration independently from the ERK1/2 signaling pathway. Invest. Ophthalmol. Vis. Sci. *57*, 56–65. https://doi.org/10.1167/iovs.15-18129.

Du, L.L., and Liu, P. (2016). CXCL12/CXCR4 axis regulates neovascularization and lymphangiogenesis in sutured corneas in mice. Mol. Med. Rep. *13*, 4987–4994. https://doi.org/10.3892/mmr.2016.5179.

Eghtedari, Y., Richardson, A., Mai, K., Heng, B., Guillemin, G.J., Wakefield, D., and Di Girolamo, N. (2016). Keratin 14 expression in epithelial progenitor cells of the developing human cornea. Stem Cell Dev. *25*, 699–711. https://doi.org/10.1089/scd.2016.0039.

Fricker, S.P., Anastassov, V., Cox, J., Darkes, M.C., Grujic, O., Idzan, S.R., Labrecque, J., Lau, G., Mosi, R.M., Nelson, K.L., et al. (2006). Characterization of the molecular pharmacology of AMD3100: a specific antagonist of the G-protein coupled chemokine receptor, Cxcr4. Biochem. Pharmacol. *72*, 588–596. https://doi.org/10.1016/j.bcp.2006.05.010.

Gerdes, J., Schwab, U., Lemke, H., and Stein, H. (1983). Production of a mouse monoclonal antibody reactive with a human nuclear antigen associated with cell proliferation. Int. J. Cancer *31*, 13–20. https://doi.org/10.1002/ijc.2910310104.

Ghareeb, A.E., Lako, M., and Figueiredo, F.C. (2020). Recent advances in stem cell therapy for limbal stem cell deficiency: a narrative review. Ophthalmol. Ther. *9*, 809–831. https://doi.org/10.1007/s40123-020-00305-2.

González, S., Oh, D., Baclagon, E.R., Zheng, J.J., and Deng, S.X. (2019). Wnt signaling is required for the maintenance of human limbal stem/progenitor cells in vitro. Invest. Ophthalmol. Vis. Sci. *60*, 107–112. https://doi.org/10.1167/iovs.18-25740.

Gouveia, R.M., Vajda, F., Wibowo, J.A., Figueiredo, F., and Connon, C.J. (2019). YAP, ΔNp63, and β-catenin signaling pathways are involved in the modulation of corneal epithelial stem cell phenotype induced by substrate stiffness. Cells *8*, 347. https://doi.org/10.3390/cells8040347.

Grueterich, M., Espana, E.M., and Tseng, S.C. (2003). Ex vivo expansion of limbal epithelial stem cells: amniotic membrane serving as a stem cell niche. Surv. Ophthalmol. *48*, 631–646. https://doi.org/10.1016/j.survophthal.2003.08.003.

Haagdorens, M., Van Acker, S.I., Van Gerwen, V., S, N.D., Koppen, C., Tassignon, M.J., and Zakaria, N. (2016). Limbal stem cell deficiency: current treatment options and emerging therapies. Stem Cell. Int. *2016*, 9798374. https://doi.org/10.1155/2016/9798374.

He, C., Li, D., Gao, J., Li, J., Liu, Z., and Xu, W. (2019). Inhibition of CXCR4 inhibits the proliferation and osteogenic potential of fibroblasts from ankylosing spondylitis via the Wnt/β-catenin pathway. Mol. Med. Rep. *19*, 3237–3246. https://doi.org/10.3892/mmr.2019.9980.

Hogerheyde, T.A., Suzuki, S., Walshe, J., Bray, L.J., Stephenson, S.A., Harkin, D.G., and Richardson, N.A. (2016). Optimization of corneal epithelial progenitor cell growth on bombyx mori silk fibroin membranes. Stem Cell. Int. *2016*, 8310127. https://doi.org/10.1155/2016/8310127.

Huang, S.M., Mishina, Y.M., Liu, S., Cheung, A., Stegmeier, F., Michaud, G.A., Charlat, O., Wiellette, E., Zhang, Y., Wiessner, S., et al. (2009). Tankyrase inhibition stabilizes axin and antagonizes Wnt signalling. Nature *461*, 614–620. https://doi.org/10.1038/nature08356.

Kandyba, E., Leung, Y., Chen, Y.B., Widelitz, R., Chuong, C.M., and Kobielak, K. (2013). Competitive balance of intrabulge BMP/Wnt signaling reveals a robust gene network ruling stem cell homeostasis and cyclic activation. Proc. Natl. Acad. Sci. U S A *110*, 1351–1356. https://doi.org/10.1073/pnas.1121312110.

Kawasaki, S., Tanioka, H., Yamasaki, K., Connon, C.J., and Kinoshita, S. (2006). Expression and tissue distribution of p63 isoforms in human ocular surface epithelia. Exp. Eye Res. *82*, 293–299. https://doi.org/10.1016/j.exer.2005.07.001.

Kim, Y.H., Cho, K.A., Lee, H.J., Park, M., Kim, H.S., Park, J.W., Woo, S.Y., and Ryu, K.H. (2019). Identification of WNT16 as a predictable biomarker for accelerated osteogenic differentiation of tonsil-derived mesenchymal stem cells in vitro. Stem Cell. Int. *2019*, 8503148. https://doi.org/10.1155/2019/8503148.

Le, Q., Xu, J., and Deng, S.X. (2018). The diagnosis of limbal stem cell deficiency. Ocul. Surf. *16*, 58–69. https://doi.org/10.1016/j.jtos.2017.11.002.

Lee, H.J., Wolosin, J.M., and Chung, S.H. (2017). Divergent effects of Wnt/β-catenin signaling modifiers on the preservation of human limbal epithelial progenitors according to culture condition. Sci. Rep. *7*, 15241. https://doi.org/10.1038/s41598-017-15454-x.

Lee, J.G., and Kay, E.P. (2011). PI 3-kinase/Rac1 and ERK1/2 regulate FGF-2-mediated cell proliferation through phosphorylation of p27 at Ser10 by KIS and at Thr187 by Cdc25A/Cdk2. Invest. Ophthalmol. Vis. Sci. *52*, 417–426. https://doi.org/10.1167/iovs.10-6140.

Li, W., Hayashida, Y., Chen, Y.T., and Tseng, S.C. (2007). Niche regulation of corneal epithelial stem cells at the limbus. Cell Res. *17*, 26–36. https://doi.org/10.1038/sj.cr.7310137.

Mendoza-Reinoso, V., and Beverdam, A. (2018). Epidermal YAP activity drives canonical WNT16/β-catenin signaling to promote keratinocyte proliferation in vitro and in the murine skin. Stem Cell Res. *29*, 15–23. https://doi.org/10.1016/j.scr.2018.03.005.

Meyers, C.A., Shen, J., Lu, A., and James, A.W. (2018). WNT16 induces proliferation and osteogenic differentiation of human perivascular stem cells. J. Orthop. *15*, 854–857. https://doi.org/10.1016/j.jor.2018.08.021.

Nakatsu, M.N., Ding, Z., Ng, M.Y., Truong, T.T., Yu, F., and Deng, S.X. (2011). Wnt/β-catenin signaling regulates proliferation of human cornea epithelial stem/progenitor cells. Invest. Ophthalmol. Vis. Sci. *52*, 4734–4741. https://doi.org/10.1167/iovs.10-6486.

Ouyang, H., Xue, Y., Lin, Y., Zhang, X., Xi, L., Patel, S., Cai, H., Luo, J., Zhang, M., Zhang, M., et al. (2014). WNT7A and PAX6 define corneal epithelium homeostasis and pathogenesis. Nature *511*, 358–361. https://doi.org/10.1038/nature13465.

Ozeki, N., Mogi, M., Hase, N., Hiyama, T., Yamaguchi, H., Kawai, R., Kondo, A., and Nakata, K. (2016). Wnt16 signaling is required for IL-1β-induced matrix metalloproteinase-13-regulated proliferation of human stem cell-derived osteoblastic cells. Int. J. Mol. Sci. *17*, 221. https://doi.org/10.3390/ijms17020221.

Rama, P., Matuska, S., Paganoni, G., Spinelli, A., De Luca, M., and Pellegrini, G. (2010). Limbal stem-cell therapy and long-term corneal regeneration. New Engl. J. Med. *363*, 147–155. https://doi.org/10.1056/NEJMoa0905955.

Schermer, A., Galvin, S., and Sun, T.T. (1986). Differentiation-related expression of a major 64K corneal keratin in vivo and in culture suggests limbal location of corneal epithelial stem cells. J. Cell Biol. *103*, 49–62. https://doi.org/10.1083/jcb.103.1.49.

Shen, X., Artinyan, A., Jackson, D., Thomas, R.M., Lowy, A.M., and Kim, J. (2010). Chemokine receptor CXCR4 enhances proliferation in pancreatic cancer cells through AKT and ERK dependent pathways. Pancreas *39*, 81–87. https://doi.org/10.1097/MPA.0b013e3181bb2ab7.

Song, Z.Y., Wang, F., Cui, S.X., and Qu, X.J. (2018). Knockdown of CXCR4 inhibits CXCL12-induced angiogenesis in HUVECs through downregulation of the MAPK/ERK and PI3K/AKT and the Wnt/β-catenin pathways. Cancer Invest. *36*, 10–18. https://doi.org/10.1080/07357907.2017.1422512.

Teh, M.T., Blaydon, D., Ghali, L.R., Briggs, V., Edmunds, S., Pantazi, E., Barnes, M.R., Leigh, I.M., Kelsell, D.P., and Philpott, M.P. (2007). Role for WNT16B in human epidermal keratinocyte proliferation and differentiation. J. Cell Sci. *120*, 330–339. https://doi.org/10.1242/jcs.03329.

Tong, W., Zeng, Y., Chow, D.H.K., Yeung, W., Xu, J., Deng, Y., Chen, S., Zhao, H., Zhang, X., Ho, K.K., et al. (2019). Wnt16 attenuates osteoarthritis progression through a PCP/JNK-mTORC1-PTHrP cascade. Ann. Rheum. Dis. *78*, 551–561. https://doi.org/10.1136/annrheumdis-2018-214200.

Trosan, P., Svobodova, E., Chudickova, M., Krulova, M., Zajicova, A., and Holan, V. (2012). The key role of insulin-like growth factor I in limbal stem cell differentiation and the corneal wound-healing

process. Stem Cell Dev. *21*, 3341–3350. https://doi.org/10.1089/scd.2012.0180.

Trounson, A., and McDonald, C. (2015). Stem cell therapies in clinical trials: progress and challenges. Cell Stem Cell *17*, 11–22. https://doi.org/10.1016/j.stem.2015.06.007.

Wang, K., Ji, W., Yu, Y., Li, Z., Niu, X., Xia, W., and Lu, S. (2018). FGFR1-ERK1/2-SOX2 axis promotes cell proliferation, epithelial-mesenchymal transition, and metastasis in FGFR1-amplified lung cancer. Oncogene *37*, 5340–5354. https://doi.org/10.1038/s41388-018-0311-3.

Wang, P., Zhang, H., Li, Z., Liu, X., Jin, Y., Lei, M., Jiao, Z., Bi, Y., and Guo, W. (2019). Low-dose radiation promotes the proliferation and migration of AGE-treated endothelial progenitor cells derived from bone marrow via activating SDF-1/CXCR4/ERK signaling pathway. Radiat. Res. *191*, 518–526. https://doi.org/10.1667/rr15200.1.

Xie, H.T., Chen, S.Y., Li, G.G., and Tseng, S.C. (2011). Limbal epithelial stem/progenitor cells attract stromal niche cells by SDF-1/CXCR4 signaling to prevent differentiation. Stem Cell. *29*, 1874–1885. https://doi.org/10.1002/stem.743.

Yu, M., Bojic, S., Figueiredo, G.S., Rooney, P., de Havilland, J., Dickinson, A., Figueiredo, F.C., and Lako, M. (2016). An important role for adenine, cholera toxin, hydrocortisone and triiodothyronine in the proliferation, self-renewal and differentiation of limbal stem cells in vitro. Exp. Eye Res. *152*, 113–122. https://doi.org/10.1016/j.exer.2016.09.008.

Zaim, M., Karaman, S., Cetin, G., and Isik, S. (2012). Donor age and long-term culture affect differentiation and proliferation of human bone marrow mesenchymal stem cells. Ann. Hematol. *91*, 1175–1186. https://doi.org/10.1007/s00277-012-1438-x.

Zheng, M., Tian, C., Fan, T., and Xu, B. (2019). Fibronectin regulates the self-renewal of rabbit limbal epithelial stem cells by stimulating the Wnt11/Fzd7/ROCK non-canonical Wnt pathway. Exp. Eye Res. *185*, 107681. https://doi.org/10.1016/j.exer.2019.05.021.

Zheng, T., and Xu, J. (2008). Age-related changes of human limbus on in vivo confocal microscopy. Cornea *27*, 782–786. https://doi.org/10.1097/ICO.0b013e31816f5ec3.